

Thermal and Mechanical Characterization of Compressed Clay Bricks Reinforced by Rice Husks for Optimizing Building in Sahelian Zone

Modjonda, Souaibou, Yanné Etienne, Danwe Raidandi

Department of Civil Engineering and Architecture, National Advanced School of Engineering of Maroua, University of Maroua, Maroua, Cameroon

Email: felixmodjonda@yahoo.fr, souelma@yahoo.fr, yanneetienne@yahoo.fr, rdanwe@yahoo.fr

How to cite this paper: Modjonda, Souaibou, Etienne, Y. and Raidandi, D. (2023) Thermal and Mechanical Characterization of Compressed Clay Bricks Reinforced by Rice Husks for Optimizing Building in Sahelian Zone. *Advances in Materials Physics and Chemistry*, **13**, 177-196.

<https://doi.org/10.4236/ampc.2023.1310013>

Received: August 21, 2023

Accepted: October 28, 2023

Published: October 31, 2023

Copyright © 2023 by author(s) and Scientific Research Publishing Inc. This work is licensed under the Creative Commons Attribution International License (CC BY 4.0).

<http://creativecommons.org/licenses/by/4.0/>



Open Access

Abstract

This article deals with the characterization of local materials used in insulation building heat. These materials are bricks of earth compressed and stabilized with rice husks. Thermal conductivity, the specific heat and the thermal diffusivity of materials based on clay incorporating rate of 0, 2%, 4%, 6%, 8% and 10% are determined. The results showed that the clay blocks + rice balls had better thermal insulators than simple clay blocks. However, these composite materials used for the envelope of the building must have sufficient mechanical resistance when used in construction. The measurement of mechanical properties such as compressive strength showed an improvement of 6% and beyond, a drop in resistance when increasing rice husks in clay is observed. These results allow to specify the optimal conditions of use of these materials for the building envelope.

Keywords

Clay Bricks, Rice Husks, Thermomechanical Characterisation, Thermal Insulation, Transient Method

1. Introduction

The increased use of non renewable resources and increased greenhouse gas emissions resulted in increasing environmental problems. The impact of building performance on the ecological environment gradually attracts more and more public attention. In the world, buildings account for approximately a third of both all energy use and greenhouse gas emissions [1] [2]. Globally, 24% of the raw materials are used in the construction industry; while the residential and

commercial buildings use 32% of total energy and account for over 30% of green gas emissions worldwide [3]. In this context, it has been reported that cement is the most widely used man made material and is the source of about 8% of the world's CO₂ emissions [4].

Today, the awareness of the global warming and necessity for energy saving on the one hand and improved indoor comfort provided by earth material on the other hand give this material the potential for construction of sustainable buildings [5] [6] [7]. For centuries, clay materials have been used in building construction, in various forms such as adobe (sun dried brick), rammed earth and recently compressed earth block (CEBs), and proved promising to provide affordable and comfortable housing. Earth-based materials may be important in this respect [8] [9].

The earth material has interesting properties. For example, they can also have thermal properties that can result in a more stable indoor environment. Earth has low thermal conductivity, contributing to thermal comfort. It is available in quantity and ubiquitous, does not emit greenhouse gases. It is fire resistant and aesthetic [10] [11] [12] [13].

However, clay brick has limited mechanical properties. In order to improve the mechanical properties, a stabilizer can be added to the earth. Nevertheless, it is advisable to choose a stabilizer appropriate to the variety of soil used. The most practiced methods are those of: densification by compression, adding fibers to the mixture, adding cement or lime to the earth or mixing the earth with bitumen [1] [7] [14]-[20].

Stabilization will act on the texture and structure of the earth, the only parameters that can be modified. It can proceed by three methods. The first is to reduce the porosity of the matrix by minimizing the volumes of voids present between particles. This method corresponds to the compression of the earth, which modifies its density, its mechanical resistance, its compressibility, its permeability and its porosity. The second is to modify the permeability of the earth by removing voids that cannot be removed. It acts on the texture of the earth by controlling the particule sizes, by subjecting it to heat treatment or even electrical treatment. The last possibility is to modify the mechanical resistance by reinforcing the bonds between particles. It corresponds to the modification of the properties of the earth by the addition of other materials or chemicals [21]-[26].

If the soil is too rich in clay, the first materials to add are sands and gravels. Indeed, they make it possible to obtain a better distributed particle size curve. Thus, shrinkage and swelling will be controlled while a better distribution of the porosity will be obtained. The density will also be higher thanks to a better cohesion between the particles of the earth. However, it will be necessary to ensure that the mixing of the materials is done in an optimal way to avoid the presence of clay clods. Pozzolans, such as some volcanic ash, can also be added to land with too much clay. Fly ash containing calcium carbonate can be used as a stabilizer in proportions varying from 5% to 10%. They improve compressive strength and reduce shrinkage and swelling. However, they have no effect on water resistance.

They can be combined with lime stabilization to obtain better results [5] [25] [27]. For proportions of 6% to 12% cement, up to 8% ash can be added, the compressive strength and water absorption of compressed earth bricks are not affected [28] [29].

Earth stabilized with fibers therefore has a very good resistance to cracking as well as to the propagation of cracks because they oppose splitting when the stress increases. If we compare the resistance of a material reinforced with fibers to the original material without fiber, we observe a higher resistance of about 15% for the material containing the fibers except in the case of a too sandy material where the fibers can have a negative effect. If we take the example of adding sheep's wool fibers to the soil, we observe an increase in compressive strength of about 37%. In the event of deformations, a greater capacity to absorb energy is also observed in the case of fiber-reinforced earth, which will be very interesting in paraseismic regions. This is explained by the fact that the fibers modify the behavior of the earth beyond the breaking point [30] [31].

There is an optimum amount of fiber to add beyond which a loss of strength is observed. Indeed, if an excessive quantity of fibers is added, the density will be too reduced and there will be insufficient contact points between the fibers and the soil. This implies that the deformations will no longer be transmitted correctly, which will reduce the resistance of the earth. Convincing results have already been obtained with a dosage of 4% by volume. The fibers are placed preferentially in all directions in order to obtain better results. The fibers can be of vegetable, animal or synthetic origin. Straws of all kinds are thus generally used, cereal husks, hemp, coconut fibers, palm fibers, etc. for vegetable fibers; cattle hair and horsehair for animal fibres; steel, fiberglass and cellophane for synthetic fibers [9] [25] [32] [33].

The search for entirely ecological materials has aroused particular interest in recent years among researchers. More recently, the suitability of clay materials should be characterized prior to the production of stabilized CEBs given that their performance is largely influenced by the characteristics of the earthen material, type and content of stabilizer as well as the production and curing process [9] [23] [34] [35] [36].

The present study investigates the suitability of clay materials for the production stabilized bricks by rice husks. This is achieved through the characterization of the thermal and mechanical properties of the clay materials. The effect of the rice husks incorporation rate clay materials was evaluated. The thermal conductivity, the bulk density and compressive strength of rice husks stabilized were considered as the main criteria for selecting the most appropriate materials for construction of buildings.

2. Materials and Methods

2.1. Materials

The earthen materials used in this study derive from Tchatibali, located at

10°2'38"N, 14°55'47"W in the Far North Region of Cameroon. It was stocked in the laboratory and directly used for mixing. The grading curves and the particle sizes of the earthen materials were determined by grain size analysis according to [32] [37] [38] [39]. The composition of the earthen material is 41% clay (less than 5 mm), 29% silt (between 5 and 50 mm) and 30% sand (between 50 and 2000 mm). The test results are presented in **Figure 1**. The Atterberg's limits are considered to assess the soil plasticity for its effective use in civil engineering [40].

Rice husks are by-products from rice harvesting. These by-products are collected and stored in the laboratory at room temperature to be and are mixed with the clay paste.

2.2. Sample Preparation

Before the preparation of compressed earthen samples, the earthen material was sieved to remove the oversized gravel (larger than 2 mm diameter) and organic matter. The sieved material was dried in air at a temperature of 105°C to obtain a constant weight. The materials used are shown in **Figure 2(a)** and **Figure 2(b)**. Samples were made by mixing rice husks with the binder material in the beater during 5 min. The mixture was mixed using a mixer type E095. The mass composition of the different samples is given in **Table 1**.

For mechanical tests, a mould of dimensions $4 \times 4 \times 31.6 \text{ cm}^3$ was used to prepare samples by a hydraulic press under a pressure of 20 to 250 kN, and the thermal tests samples were prepared in a mould of dimensions $10 \times 10 \times 2 \text{ cm}^3$. After compaction, the samples were placed in controlled laboratory conditions for 14 days to avoid cracking. The environmental temperature and relative humidity in the laboratory during the drying process were 27°C and 60%, respectively. **Figure 3(a)** and **Figure 3(b)** showed respectively sample for thermal test and mechanical test.

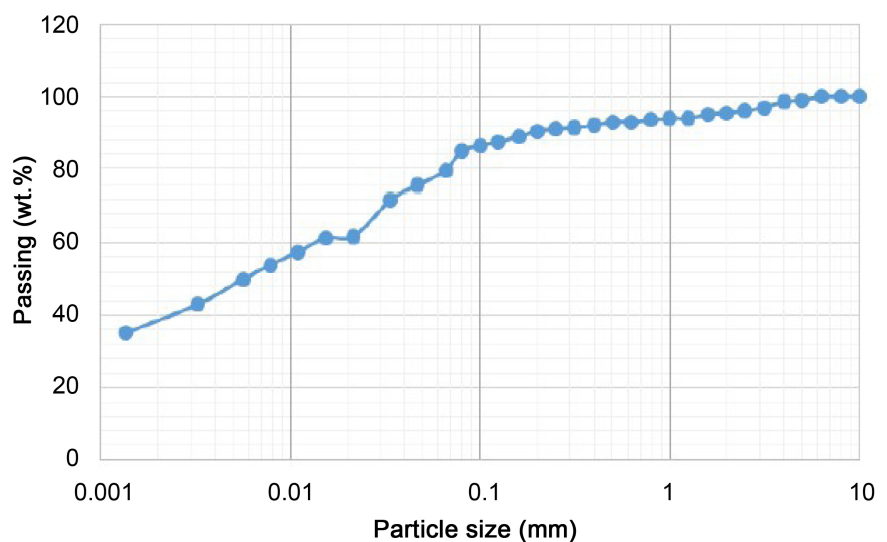


Figure 1. Particle size curve of the clay studied.



Figure 2. Materials used for analysis: (a) Clay sample from the site; (b) Rice husks.

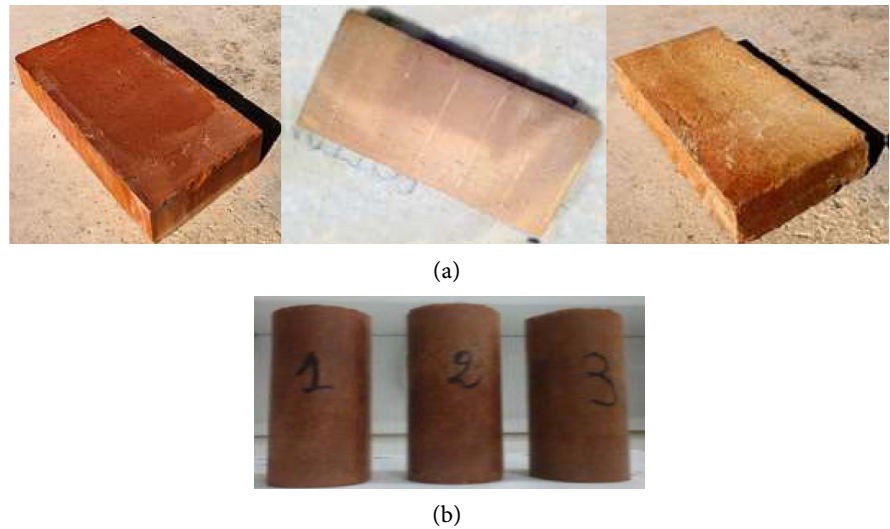


Figure 3. Samples for different tests. (a) Samples for thermal test. (b) Samples for mechanical test.

Table 1. Composition of the different samples.

Samples	Binder percentage (%)	Binder mass (g)	Rice huscks mass (g)	Water mass (g)
C1	100	200	0	82.12
C2	98	196	4	89.35
C3	96	192	8	99.23
C4	94	188	12	114.69
C5	92	184	16	136.04
C6	90	180	20	145.18

2.3. Mechanical Characterization

Mechanical characterization consists in the determination of the compression resistance. Test was performed with three specimens for each mixture. This characterization was done using an E0160 type mechanical press with a maximum force of 70 kN and 0.05 kN of precision. The specific speed of the force applica-

tion was 2 kN/s. For the determination of the compression resistance, the prismatic sample described in 2.2 was placed in the press as represented schematically in **Figure 4**. The mechanical tests consist in applying a force F on the standardized sample and measuring its strain on breaking point. The maximum stress which the sample can bear before breaking is the tensile strength or the compression resistance. It is defined by (1):

$$\sigma = \frac{F}{S} \quad (1)$$

S is the sample section in mm^2 , F is the force applied (N) and σ is the stress in MPa.

2.4. Thermophysical Characterization

The testing tool used to show the thermophysical characterisation is the asymmetric hot plane method [41] [42]. It's a transient characterization approach used to get the apparent thermal conductivity of a material by estimating the thermal effusivity E and the volumetric heat capacity ρC_p in relation to the testing temperature $T_{exp}(t)$ and modelled temperature $T_{mod}(t)$. The testing instruments used for measuring the thermal properties are shown in **Figure 5**.

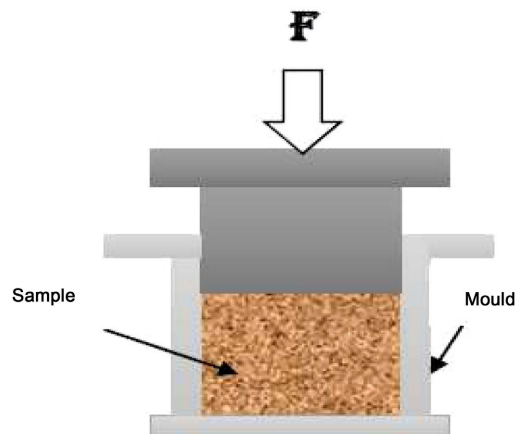


Figure 4. Schema of the compression test.



Figure 5. The testing instruments used for measuring the thermal properties.

Material with specifications of $10 \times 10 \times 2 \text{ cm}^3$ is placed on a heat sensor between two polystyrene blocks of $10 \times 10 \times 5 \text{ cm}^3$. A generator is used to heat the resistor. The increase in temperature at the centre of the heat resistor was as a result of type K thermocouple that registers the test temperature on the hot surface of the material. The experimental temperatures $T_{exp}(t)$ were registered using the acquisition module TC 08-USB Picolog. The dropping of experimental and simulated temperature obtained after modelling the testing instrument helped us to estimate E and ρC_p . It is therefore important to note that the temperature above the polystyrene blocks remains at its initial state, to arrive at this; we placed two aluminium blocks of $10 \times 10 \times 2 \text{ cm}^3$ above and below the polystyrene blocks.

Quadrupoles Formalism of Heat Transfer

Since the transverse dimensions of the resistor are large compared to the thickness of the sample, the heat transfer can be assumed to remain unidirectional at the centre of the probe and modelled using the quadrupole method [27] [42] [43] [44]. With this assumption, the temperature at the centre of the heating element depends only on the z -coordinates and the time t .

➤ 1D model for a semi-infinite model

In this case, the thermal quadrupole method [44] can be used to solve the thermal transfer problem. Indeed, in Laplace's space, the heat equation depends only on the space variable. The method makes it possible then to relate the input and output flows and temperatures using a passing matrix. Considering the sample and polystyrene insulating block as a semi-infinite medium and hoping that the heating sensor is a thin device (Figure 6), the equations can be written following the thermal flow traces across the sample (2) or across the heating block (3):

$$\begin{bmatrix} \theta_s \\ \Phi_{hs} \end{bmatrix} = \begin{bmatrix} 1 & 0 \\ \rho_h c_h e_h S p & 1 \end{bmatrix} \begin{bmatrix} 1 & SR_{hs} \\ 0 & 1 \end{bmatrix} \begin{bmatrix} \theta_1 \\ E\sqrt{p}\theta_1 \end{bmatrix} \quad (2)$$

$$\begin{bmatrix} \theta_s \\ \phi_{hpo} \end{bmatrix} = \begin{bmatrix} A_{po} & B_{po} \\ C_{po} & D_{po} \end{bmatrix} \begin{bmatrix} \theta_2 \\ E_{po}\sqrt{p}\theta_2 \end{bmatrix} \quad (3)$$

$$\text{With: } A_{po} = D_{po} = \cosh\left(\frac{E_{po}}{\lambda_{po}}\sqrt{p}e_{po}\right); \quad B_{po} = \frac{\sinh\left(\frac{E_{po}}{\lambda_{po}}\sqrt{p}e_{po}\right)}{E_{po}S\sqrt{p}};$$

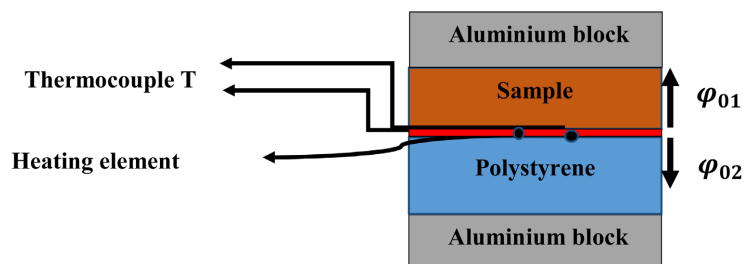


Figure 6. Across of the heat flow.

$$C_{po} = E_{po} S \sqrt{p} \sinh \left(\frac{E_{po}}{\lambda_{po}} \sqrt{p} e_{po} \right).$$

ρ_h and, c_h are respectively the density (kg/m³) and the mass heat capacity (J·kg⁻¹·K⁻¹), of the sample, λ is a thermal conductivity (W·m⁻¹·K⁻¹) of the sample, e_h the thickness (m) of the sample and S is the section (mm²) of sample and polystyrene; $C_h = \rho_h c_h e_h S$ is the thermal capacity of the sample per area unit; R_{hs} the thermal contact resistance between the heating element and the sample; Φ_{hs} the Laplace transform of the heat flux density living the heating element (upstream); ϕ_{hpo} the Laplace transform of the heat flux density living the heating element (downstream); E and E_{po} are respectively thermal effusivity of sample and polystyrene blocks while p is the Laplace parameter; \mathcal{L} the Laplace transform of the temperature $T_s(t)$.

Combining (2) and (3) yields to:

$$\theta_s(z, t) = \Phi(0, t) \frac{1}{\frac{\rho_h c_h e_h p + (1 + R_{hs} \rho_h c_h e_h S p) E \sqrt{p}}{1 + R_{hs} E S \sqrt{p}} + \frac{E_{po} \sqrt{p}}{1 + R_{hpo} E_{po} S \sqrt{p}}} \quad (4)$$

A simplified estimation at long times ($p \rightarrow 0$) of the Relation (4) allows to obtain in real space (5):

$$\Delta T(0, t \rightarrow 0) = \varphi S \left(\frac{E^2 R_{hs} + E_{po}^2 R_{hpo}}{(E + E_{po})^2} - \frac{\rho_h c_h e_h}{S (E + E_{po})^2} \right) + \frac{2\varphi}{(E + E_{po}) \sqrt{\pi}} \sqrt{t} \quad (5)$$

The numerical calculation of the slope α of the curve $= f(t^{1/2})$, which allows to obtain a pre-estimate of the thermal effusivity of the material given by the Relation (6).

$$E = E_{pre} = \frac{2\varphi}{\beta \sqrt{\pi}} - E_{po} \quad (6)$$

The heat transfer δq through the probe during an dt infinitesimally small time interval corresponds to a heat flow $\rho_0 = \frac{\delta q}{dt}$, which causes a temperature rise dT in the probe. The exploitation of the linear part of the thermogram $T = f(t)$ may be approximated from the slope β of the linear part of the curve $T(t) = f(t)$ when $T_{exp}(t)$ and $T_{sim}(t)$ are overlapped and thus the pre-estimated value of the volume heat capacity ρC_p of the sample can be deduced by the relationship (7).

$$(\rho C_p)_{pres} = \frac{1}{e_s} \left(\frac{\varphi}{\beta} - \varphi_{po} C_{po} e_{po} - \rho_h c_h e_h \right) \quad (7)$$

The pre-estimates of E and ρC_p will allow us to determine the apparent thermal conductivity of the materials by the Relation (8).

$$\lambda_{pres} = \frac{(E)_{pre}^2}{(\rho C_p)_{pres}} \quad (8)$$

➤ Asymmetric 1D quadrupole models for the complete model Temperature at

the centre of the probe.

With the Complete model, the quadrupole method no longer uses the sample and insulating block as in semi-infinite medium. Consequently:

❖ for the upward flow:

$$\begin{aligned} \begin{bmatrix} \theta_c \\ \Phi_{hs} \end{bmatrix} &= \begin{bmatrix} 1 & 0 \\ \rho_h c_h e_h S p & 1 \end{bmatrix} \begin{bmatrix} 1 & SR_{hs} \\ 0 & 1 \end{bmatrix} \begin{bmatrix} A_s & B_s \\ C_s & D_s \end{bmatrix} \begin{bmatrix} 1 & SR_{spo} \\ 0 & 1 \end{bmatrix} \begin{bmatrix} A_{po} & B_{po} \\ C_{po} & D_{po} \end{bmatrix} \begin{bmatrix} 0 \\ \Phi_m \end{bmatrix} \\ &= \begin{bmatrix} A & B \\ C & D \end{bmatrix} \begin{bmatrix} 0 \\ \Phi_1 \end{bmatrix} \end{aligned} \quad (9)$$

$$\text{With: } A_s = D_s = \cosh\left(\frac{\rho C_p}{E} \sqrt{pe}\right), \quad B_s = \frac{\sinh\left(\frac{\rho C_p}{E} \sqrt{pe}\right)}{\lambda \frac{\rho C_p}{E} \sqrt{p}}, \text{ and}$$

$$C_s = \lambda \frac{\rho C_p}{E} \sqrt{p} \sinh\left(\frac{\rho C_p}{E} \sqrt{pe}\right).$$

❖ for the downstream:

$$\begin{bmatrix} \theta_c \\ \Phi_{hpo} \end{bmatrix} = \begin{bmatrix} 1 & SR_{hpo} \\ 0 & 1 \end{bmatrix} \begin{bmatrix} A_{po} & B_{po} \\ C_{po} & D_{po} \end{bmatrix} \begin{bmatrix} 0 \\ \Phi_2 \end{bmatrix} \quad (10)$$

The total heat flux density in the Laplace field is calculated from relation (11):

$$\Phi_0 = \Phi_1 + \Phi_2 \quad (11)$$

Combining Relations (3), (9) and (11), we then obtain the expression for the temperature at the centre of the probe in Laplace space, given by Relation (12).

$$\theta_c(z, p) = \frac{B_{po} B_s}{D_s B_{po} + D_{po} B_s} \Phi(0, p) \quad (12)$$

The temperature $T(t)$ in real space is obtained by inverse Laplace transformation (13):

$$T(t) = L^{-1}[\theta_c(p)] \quad (13)$$

by using Stehfest's method [45] [46] [47] [48]. The Levenberg-Marquart algorithm [49] [50] [51], integrated in a Matlab code, allows us to estimate the value of E that minimizes the sum of the squared errors of the functional:

$$\psi = \sum_{i=0}^n [\Delta T_{exp}(t_i) - \Delta T_{mod}(t_i)]^2 \quad (14)$$

between the experimental curve:

$$\Delta T_{c\ exp}(t) = T_{c\ exp}(0, t) - T_{c\ exp}(e, t) \quad (15)$$

and the theoretical 1D curve:

$$T_{c\ mod}(t) = T_{c\ mod}(0, t) \quad (16)$$

3. Experimental Results

3.1. Mechanical Results

The mechanical results concerned the mechanical resistance to compression.

Figure 7 presents the variation of these resistances in terms of the binder percentage. The compressive strength of adobe bricks without stabilizer is 2.5 MPa, which has a close value to the compressive strength obtained by C. Babé *et al.* [8] on adobes alone. This compressive strength (3 MPa) is better than that of reinforced with 0, 2%, 4%, 8% and 10% fiber (2.5, 2, 1.8, 2.6 and 2.4 MPa respectively).

The increase in compressive strength is 20%, compared to the raw adobe. Thus, the optimal fiber content giving the maximum compressive strength of the adobes is 6% of the fiber content. In this case, an increase in compressive strength is obtained because adobes are more resistant to loads according to the literature [52] [53] [54]. Likewise, at this percentage, the fibers strengthen and maintain the solid matrix, increase the bonding strength of the earth-fiber mixture and the appearance of cracks is greatly reduced [55] [56].

On the other hand, for the other specimens (0, 2%, 4%, 8% and 10%), the addition of rice husks rather contributed to the reduction of the mechanical properties. In the same way, similar mechanical characteristics are observed by other authors [57] [58]. This similarity in the reduction of mechanical strength which remains below the maximum strength is attributed to the weak bond of the fibers with the clay matrix. This could be due to a less satisfactory bond between the fibers and the clay matrix.

According to the African standard, earth bricks with a compressive strength between 2 and 4 MPa are used in non-load-bearing walls.

3.2. Thermal Characteristics of Bricks

3.2.1. Sensitivity Study

The asymmetric hot-plane method makes possible the estimation thermal diffusivity and thermal conductivity as long as the fundamental assumption of 1D transfer is verified [35] [49] [59]. **Figure 8** shows that agreement obtained between the experimental and the theoretical curves is very good. This illustration

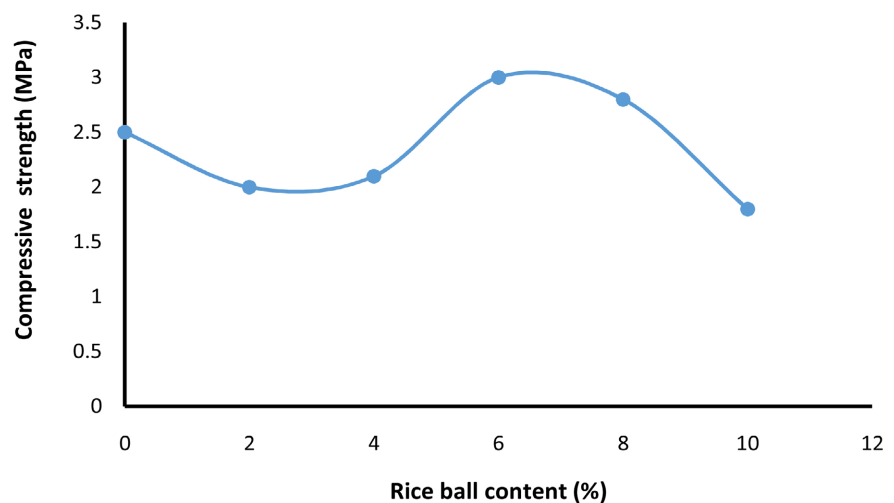


Figure 7. Compressive strengths as function of rice husks (%).

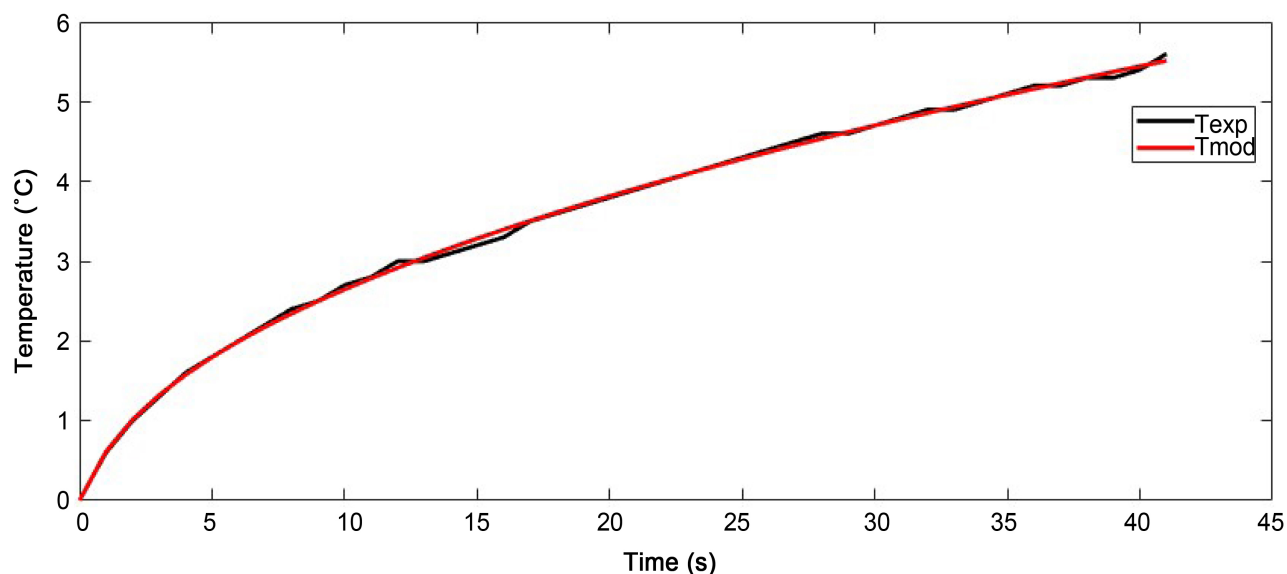


Figure 8. Experimental and simulated curves.

confirmed previous studies which indicate that this method is well suited for the measurement of thermal parameters of solid insulating materials of moderate thickness [8]. This shows that the transfer remains unidirectional for the duration of the test. Consequently, the quadrupole model developed is valid for the estimation of thermophysical parameters. Allow that, the model developed is reliable for the precise estimation of thermal conductivity. The results are similar to those published by other authors [25] [33].

The temperature only becomes sensitive to the thermal conductivity of the material from the time t_1 when the hypothesis of the semi-infinite space is no longer valid. This time t_1 corresponds to approximately 20 s for the above experiment. Furthermore, the heat exchanges on the lateral side impose a convective 3D transfer, including in the center from a certain time t_2 . If the time t_1 is greater than the time t_2 , it will be impossible to estimate the thermal conductivity of the sample because the heat transfer including at the center will be 3D before the temperature becomes sensitive to the conductivity. Probe inertia and contact resistance don't influence the temperature at long times.

The reduced sensitivities of the temperature of parameter E , ρC and Rc were calculated as presented in **Figure 9**. Parameter measurement can be performed as soon as their curve is decorated. This condition is fulfilled when the theoretically calculated temperature curve coincides with the experimental temperature curve (see **Figure 8** & **Figure 9**).

3.2.2. Thermal Conductivity

Thermal conductivity is an essential characteristic in the appreciation of the energy efficiency that a material can offer. **Figure 10** illustrates the evolution of thermal conductivity as a function of rice husk.

The results show that the apparent thermal conductivity of composite material

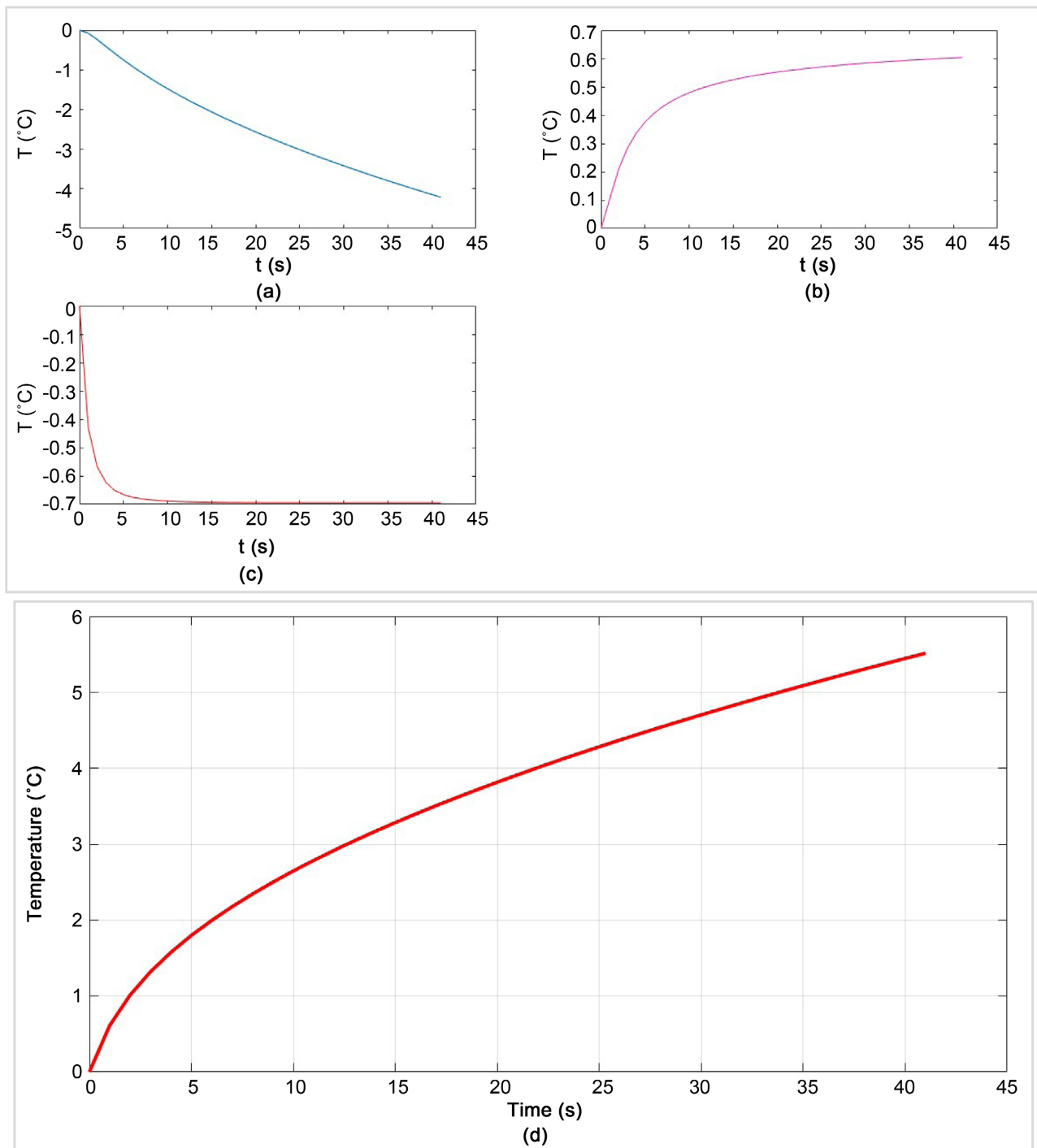


Figure 9. Sensitivity of the parameters.

decreases with increasing concentration of plant material. The thermal conductivity of clay bricks reinforced with rice husks are 0.93; 0.85; 0.72; 0.66; 0.54 and 0.37 W/(m·k) for organic residue content of 0, 2%, 4%, 6%, 8% and 10% respectively. A decrease in thermal conductivity of 39.78% is observed when increasing the rice husks by 0 to 10% compared to the sample without vegetable matter. This decrease in thermal conductivity may be due to the bulk density (**Table 2**).

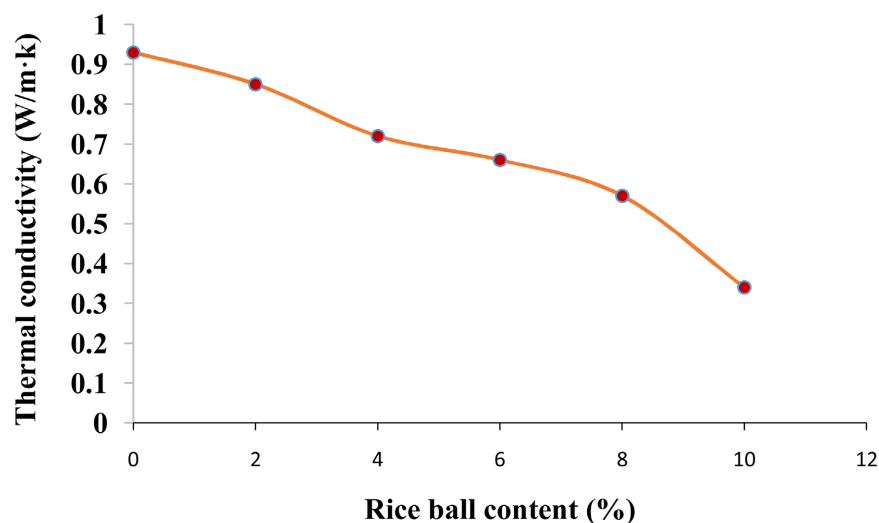


Figure 10. Thermal conductivity of bricks as a function of rice husks (%).

Table 2. Thermal properties of different samples.

Sample	λ ($\text{W}\cdot\text{m}^{-1}\cdot\text{K}^{-1}$)	ρc ($\text{J}\cdot\text{m}^{-3}\cdot\text{K}^{-1}$)	α ($\text{m}^2\cdot\text{s}^{-1}$)	ρ (kg/m^3)
Bricks + 0% rice ball	0.93	1.94×10^6	4.80×10^{-5}	1875
Bricks + 2% rice ball	0.85	1.95×10^6	4.35×10^{-5}	1810
Bricks + 4% rice ball	0.72	1.95×10^6	3.69×10^{-5}	1734
Bricks + 6% rice ball	0.66	1.96×10^6	3.36×10^{-5}	1678
Bricks + 8% rice ball	0.54	1.97×10^6	2.98×10^{-5}	1612
Bricks + 10% rice ball	0.37	1.97×10^6	1.88×10^{-5}	1567

Moreover, since rice husk are lighter, the gradual replacement of the ground volume by the vegetable matter promotes the decrease in thermal conductivity [8] [60] [61]. The apparent density of the samples varied between $1910 \text{ kg}/\text{m}^3$ for the pure dry brick and $1854 \text{ kg}/\text{m}^3$ for the dry brick with the maximum rice husk mass content. The correspondent the values of the thermal conductivities varied between 0.93 and $0.37 \text{ W}/(\text{m}\cdot\text{K})$ respectively. This result proves the interest of adding rice husks to contribute to the decrease in thermal conductivity of clay bricks. These values are similar to those obtained by other authors who have shown that beyond 6%, the porosity is high and the matrix soil has weak mechanical characteristics, thus influencing its use as bricks in the building construction [62].

3.2.3. Thermal Diffusivity

The specific heat C_{exp} is calculated from the heat capacity $(\rho C)_{exp}$ measured using the hot plate device and the density. Figure 11 shows a different value of bricks as in terms of rice husk.

The results show a linear increase in specific heat as a function of the percentage of rice husks in the brick. These values are respectively 1035; 1080; 1126; 1170;

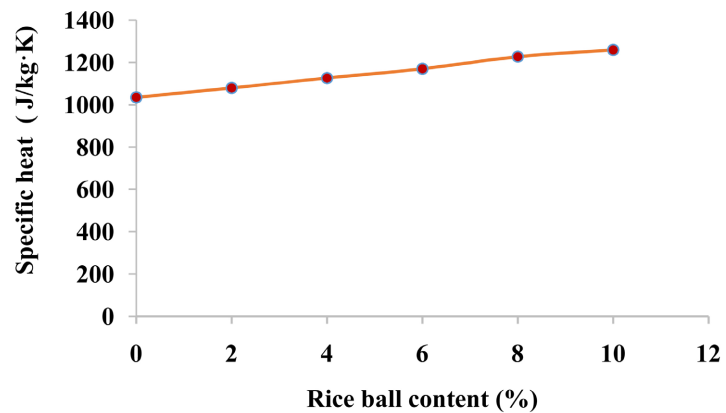


Figure 11. Specific heat of bricks as a function of rice husks (%).

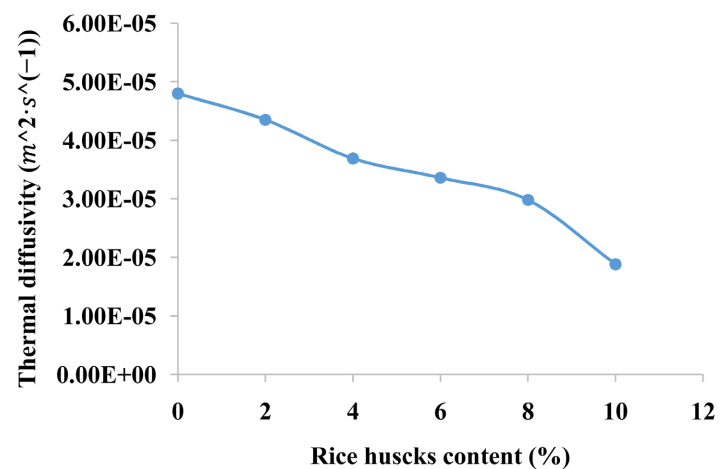


Figure 12. Thermal diffusivity of bricks as a function of rice husks (%).

1227 and 1259 J·kg⁻¹·K⁻¹ for additions of 0, 2%, 4%, 6%, 8% and 10% rice husks. The specific heat of a body (or specific heat capacity) being the quantity of energy to be supplied to raise the temperature of the unit of mass of the body by one kelvin, we observe a variation of 17% of the specific heat between pure brick and brick containing 10% of agricultural residues. These results are in agreement with other authors who show that the more the material is insulating, the more the material absorbs heat [8] [63] [64]. The specific heat capacity of adobes increases when their density decreases, since the fibers plants have a higher capacity than mineral elements.

3.2.4. Thermal Diffusivity

Figure 12 shows that the evolution of the thermal diffusivity follows the same variation as the thermal conductivity, it decreases with the increase in the percentage of addition. An insulating material, in addition to its low thermal conductivity, it must have a good ability to delay the transmission of heat flow [65].

In **Figure 8**, it can be seen that the thermal diffusivity decreases with the addition of rice husks. A drop of 39.1% in thermal diffusivity between the reference brick ($4.80 \times 10^{-5} \text{ m}^2\cdot\text{s}^{-1}$) and that having 10% rice husks ($1.88 \times 10^{-5} \text{ m}^2\cdot\text{s}^{-1}$) is

obtained. This decrease is due to the hollow structure of rice husks and their morphologies which act on the heat transmission inside the composite and subsequently they serve to reduce the diffusivity and thermal conductivity of composite.

The porosity rate, the percentages of fiber addition and the composition of materials are all factors that influence the thermal performance of composite. An insulating material, in addition to its low thermal conductivity, must have a good ability to delay the transmission of heat flow [66] [67].

4. Conclusions and Recommendations

An interesting Perseus is the use of rice husk in the manufacture of clay bricks. It is part of a sustainable development approach and has the advantage of using a renewable raw material unlike aggregates from quarries whose resources depleted. We have shown in this work that the addition of organic matter in the raw material decreases the density of the brick. Bricks, under this effect, become more heritage and help to lower dead loads in buildings. The use of lightweight bricks reduces transportation expenses and the cost of walls.

The addition of rice husks creates pores in the finished product. Higher porosity is a sought-after feature today in order to save energy because the presence of pore in the materials contributes to reducing the thermal conductivity and thus increasing its insulating power.

In view of the results obtained, it can be seen that the thermal insulation of the bricks manufactured with 6% husck gives better compressive strength. Incorporating rice husks into clay improves thermal insulation. Experimental results indicate that bricks with better thermal insulation have acceptable resistances. Numerical studies will allow reinforce the experimental results and give arguments the choice of stabilized earth bricks in the construction elements.

In perspective, it would be interesting to set up a numerical model capable to predict and simulate the behavior of rice husck-based materials. Lightweight aggregate concretes offer an alternative compared to conventional materials which are sometimes very expensive and less suitable for construction in tropical areas.

In addition, a study of the evolution of the heat effusivity of the material for a given rice husck content as a function of the water content in order to verify the linearity between these two parameters is under processing.

Conflicts of Interest

The authors declare no conflicts of interest regarding the publication of this paper.

References

- [1] Zhang, L., Yang, L., Jelle, B.P., Wang, Y. and Gustavsen, A. (2018) Hygrothermal Properties of Compressed Earthen Bricks. *Construction and Building Materials*, **162**, 576-583. <https://doi.org/10.1016/j.conbuildmat.2017.11.163>
- [2] Dime, T., Sore, S.O., Nshimiyimana, P., Messan, A. and Courard, L. (2022) Com-

- parative Study of the Reactivity of Clay Earth Materials for the Production of Compressed Earth Blocks in Ambient Conditions: Effect on Their Physico-Mechanical Performances. *Journal of Minerals and Materials Characterization and Engineering*, **10**, 43-56. <https://doi.org/10.4236/jmmce.2022.101004>
- [3] Tetey, U.Y.A., Dodoo, A. and Gustavsson, L. (2017) Energy Use Implications of Different Design Strategies for Multi-Storey Residential Buildings under Future Climates. *Energy*, **138**, 846-860. <https://doi.org/10.1016/j.energy.2017.07.123>
- [4] Roshan, G.R., Oji, R. and Attia, S. (2019) Projecting the Impact of Climate Change on Design Recommendations for Residential Buildings in Iran. *Building and Environment*, **155**, 283-297. <https://doi.org/10.1016/j.buildenv.2019.03.053>
- [5] Kurmus, H. and Mohajerani, A. (2020) Recycling of Cigarette Butts in Fired Clay Bricks: A New Laboratory Investigation. *Materials*, **13**, Article 790. <https://doi.org/10.3390/ma13030790>
- [6] Bessa, A., Bigas, J. and Gallias, J. (2004) Evaluation of the Binding Contribution of Mineral Additions to the Porosity, Compressive Strength and Durability Mortars.
- [7] Moriarty, J.P. and Svare, T.I. (1976) Housing Materials and Methods for Tropical Africa. *Batiment International, Building Research and Practice*, **4**, 28. <https://doi.org/10.1080/09613217608550444>
- [8] Babé, C., et al. (2020) Thermomechanical Characterization and Durability of Adobes Reinforced with Millet Waste Fibers (*Sorghum bicolor*). *Case Studies in Construction Materials*, **13**, e00422. <https://doi.org/10.1016/j.cscm.2020.e00422>
- [9] Kossi Imbga, B., Bodian, S., Toure, P.M., Dieye, Y. and Sambou, V. (2022) Study of the Thermochemical and Mechanical Properties of Laterite Bricks Stabilised with Cements. *International Journal of Advanced Research*, **10**, 589-603. <https://doi.org/10.21474/IJAR01/15878>
- [10] Muñoz, P., Letelier, V., Bustamante, M.A., Marcos-Ortega, J. and Sepúlveda, J.G. (2020) Assessment of Mechanical, Thermal, Mineral and Physical Properties of Fired Clay Brick Made by Mixing Kaolinitic Red Clay and Paper Pulp Residues. *Applied Clay Science*, **198**, Article ID: 105847. <https://doi.org/10.1016/j.clay.2020.105847>
- [11] Izard, J., Lelong, J., Materiaux, L.E.S. and Inertie, E.T.L. (2010) Les Matériaux Et L'Inertie Thermique.
- [12] El Boukili, G., Lechheb, M., Ouakarrouh, M., Dekayir, A., Kifani-Sahban, F. and Khaldoun, A. (2021) Mineralogical, Physico-Chemical and Technological Characterization of Clay from Bensmim (Morocco): Suitability for Building Application. *Construction and Building Materials*, **280**, Article ID: 122300. <https://doi.org/10.1016/j.conbuildmat.2021.122300>
- [13] El Fgaier, F., Lafhaj, Z., Chapiseau, C. and Antczak, E. (2016) Effect of Sorption Capacity on Thermo-Mechanical Properties of Unfired Clay Bricks. *Journal of Building Engineering*, **6**, 86-92. <https://doi.org/10.1016/j.jobbe.2016.02.011>
- [14] Moriarty, P. (1979) The Case for Traditional Housing in Tropical Africa. *Habitat International*, **4**, 285-290. [https://doi.org/10.1016/0197-3975\(79\)90038-9](https://doi.org/10.1016/0197-3975(79)90038-9)
- [15] Costa, R. (1989) Architecture in Black Africa between Development and Tradition. *Solar & Wind Technology*, **6**, 383-387. [https://doi.org/10.1016/0741-983X\(89\)90057-X](https://doi.org/10.1016/0741-983X(89)90057-X)
- [16] Coch, H. (1998) Bioclimatism in Vernacular Architecture. *Renewable and Sustainable Energy Reviews*, **2**, 67-87. [https://doi.org/10.1016/S1364-0321\(98\)00012-4](https://doi.org/10.1016/S1364-0321(98)00012-4)
- [17] Ma, S., Wu, Y. and Bao, P. (2021) Experimental Study on the Properties of Modern

- Blue Clay Brick for Kaifeng People's Conference Hall. *Scientific Reports*, **11**, Article No. 20631. <https://doi.org/10.1038/s41598-021-00191-z>
- [18] Liu, J. and Zhang, Z. (2020) Characteristics and Weathering Mechanisms of the Traditional Chinese Blue Brick from the Ancient City of Ping Yao. *Royal Society Open Science*, **7**, Article ID: 200058. <https://doi.org/10.1098/rsos.200058>
- [19] Chapagain, Y.P., Sapkota, S., Ghale, D.B., Bohara, N.B., Duwal, N. and Bhattarai, J. (2020) A Case Study on Mineralogy and Physico-Mechanical Properties of Commercial Bricks Produced in Nepal. *SN Applied Sciences*, **2**, Article No. 1856. <https://doi.org/10.1007/s42452-020-03535-y>
- [20] Asdrubali, F., D'Alessandro, F. and Schiavoni, S. (2015) A Review of Unconventional Sustainable Building Insulation Materials. *Sustainable Materials and Technologies*, **4**, 1-17. <https://doi.org/10.1016/j.susmat.2015.05.002>
- [21] Kagonbé, B.P., Tsozué, D., Nzeukou, A.N. and Ngos III, S. (2021) Mineralogical, Geochemical and Physico-Chemical Characterization of Clay Raw Materials from Three Clay Deposits in Northern Cameroon. *Journal of Geoscience and Environment Protection*, **9**, 86-99. <https://doi.org/10.4236/gep.2021.96005>
- [22] Khourchid, A.M., Ajjur, S.B. and Al-Ghamdi, S.G. (2022) Building Cooling Requirements under Climate Change Scenarios: Impact, Mitigation Strategies, and Future Directions. *Buildings*, **12**, Article 1519. <https://doi.org/10.3390/buildings12101519>
- [23] Dieye, Y., Sambou, V., Faye, M., Thiam, A., Adj, M. and Azilinson, D. (2017) Thermo-Mechanical Characterization of a Building Material Based on Typha Australis. *Journal of Building Engineering*, **9**, 142-146. <https://doi.org/10.1016/j.jobe.2016.12.007>
- [24] Bouchefra, I., EL Bichri, F.Z., Chehouani, H. and Benhamou, B. (2022) Mechanical and Thermophysical Properties of Compressed Earth Brick Reinforced by Raw and Treated Doum Fibers. *Construction and Building Materials*, **318**, Article ID: 126031. <https://doi.org/10.1016/j.conbuildmat.2021.126031>
- [25] Nitcheu, M., Meukam, P., Damfeu, J.C. and Njomo, D. (2018) Thermomechanical Characterisation of Compressed Clay Bricks Reinforced by Thatch Fibres for the Optimal Use in Building. *Materials Sciences and Applications*, **9**, 913-935. <https://doi.org/10.4236/msa.2019.912066>
- [26] Lahdili, M., El Abbassi, F.E., Sakami, S. and Aamouche, A. (2022) Mechanical and Thermal Behavior of Compressed Earth Bricks Reinforced with Lime and Coal Aggregates. *Buildings*, **12**, Article 1730. <https://doi.org/10.3390/buildings12101730>
- [27] Meukam, P., Jannot, Y., Noumowe, A. and Kofane, T.C. (2004) Thermo Physical Characteristics of Economical Building Materials. *Construction and Building Materials*, **18**, 437-443. <https://doi.org/10.1016/j.conbuildmat.2004.03.010>
- [28] Giuffrida, G., Caponetto, R. and Nocera, F. (2019) Hygrothermal Properties of Raw Earth Materials: A Literature Review. *Sustainability*, **11**, Article 5342. <https://doi.org/10.3390/su11195342>
- [29] Sadouri, R. (2022) Elaboration and Characterization of Earth-Sand Adobe Bricks Reinforced by Alfa Fibers. <https://doi.org/10.21203/rs.3.rs-1902393/v1>
- [30] Asheghi, R., Abbaszadeh Shahri, A. and Khorsand Zak, M. (2019) Prediction of Uniaxial Compressive Strength of Different Quarried Rocks Using Metaheuristic Algorithm. *Arabian Journal for Science and Engineering*, **44**, 8645-8659. <https://doi.org/10.1007/s13369-019-04046-8>
- [31] Nasiri, H., Homafar, A. and Chelgani, S.C. (2021) Prediction of Uniaxial Compressive Strength and Modulus of Elasticity for Travertine Samples Using an Explaina-

- ble Artificial Intelligence. *Results in Geophysical Sciences*, **8**, Article ID: 100034. <https://doi.org/10.1016/j.ringps.2021.100034>
- [32] Ouedraogo, M., et al. (2019) Physical, Thermal and Mechanical Properties of Adobes Stabilized with Fonio (*Digitaria exilis*) Straw. *Journal of Building Engineering*, **23**, 250-258. <https://doi.org/10.1016/j.jobe.2019.02.005>
- [33] Eric, K.K., et al. (2022) Thermophysical and Mechanical Characterization of Poto-Poto Compressed Blocks for Use as Fill Material. *Materials Sciences and Applications*, **12**, 437-459. <https://doi.org/10.4236/msa.2021.1210029>
- [34] Moussa, P., Sambou, V., Faye, M., Thiam, A. and Adj, M. (2018) Mechanical and Hygrothermal Properties of Compressed Stabilized Earth Bricks (CSEB). *Journal of Building Engineering*, **13**, 266-271. <https://doi.org/10.1016/j.jobe.2017.08.012>
- [35] Mor Diarra Ndiaye, M., Touré, P.M., Dieye, Y. and Gueye, P.M. (2019) Thermo-Mechanical Characterization of Building Component with Crushed Millet Stalk Fiber. *International Journal of Innovation and Applied Studies*, **26**, 1230-1239.
- [36] Ben Mansour, M., Jelidi, A., Cherif, A.S. and Ben Jabrallah, S. (2016) Optimizing Thermal and Mechanical Performance of Compressed Earth Blocks (CEB). *Construction and Building Materials*, **104**, 44-51. <https://doi.org/10.1016/j.conbuildmat.2015.12.024>
- [37] Ouedraogo, M., Bamogo, H., Sanou, I., Mazars, V., Aubert, J.E. and Millogo, Y. (2023) Microstructural, Physical and Mechanical Characteristics of Adobes Reinforced with Sugarcane Bagasse. *Buildings*, **13**, Article 117. <https://doi.org/10.3390/buildings13010117>
- [38] Malbila, E., Delvoie, S., Toguyeni, D., Attia, S. and Courard, L. (2020) An Experimental Study on the Use of Fonio Straw and Shea Butter Residue for Improving the Thermophysical and Mechanical Properties of Compressed Earth Blocks. *Journal of Minerals and Materials Characterization and Engineering*, **8**, 107-132. <https://doi.org/10.4236/jmmce.2020.83008>
- [39] Gandia, R.M., Corrêa, A.A.R., Gomes, F.C., Marin, D.B. and Santana, L.S. (2019) Physical, Mechanical and Thermal Behavior of Adobe Stabilized with "Synthetic Termite Saliva". *Engenharia Agrícola*, **39**, 139-149. <https://doi.org/10.1590/1809-4430-eng.agric.v39n2p139-149/2019>
- [40] Bertelsen, I.M.G., Belmonte, L.J., Fischer, G. and Ottosen, L.M. (2021) Influence of Synthetic Waste Fibres on Drying Shrinkage Cracking and Mechanical Properties of Adobe Materials. *Construction and Building Materials*, **286**, Article ID: 122738. <https://doi.org/10.1016/j.conbuildmat.2021.122738>
- [41] Bal, H., Jannot, Y., Gaye, S. and Demeurie, F. (2013) Measurement and Modelisation of the Thermal Conductivity of a Wet Composite Porous Medium: Laterite Based Bricks with Millet Waste Additive. *Construction and Building Materials*, **41**, 586-593. <https://doi.org/10.1016/j.conbuildmat.2012.12.032>
- [42] Damfeu, J.C., Meukam, P. and Jannot, Y. (2016) Modeling and Measuring of the Thermal Properties of Insulating Vegetable Fibers by the Asymmetrical Hot Plate Method and the Radial Flux Method: Kapok, Coconut, Groundnut Shell Fiber and Rattan. *Thermochimica Acta*, **630**, 64-77. <https://doi.org/10.1016/j.tca.2016.02.007>
- [43] Antar, M.A. (2010) Thermal Radiation Role in Conjugate Heat Transfer across a Multiple-Cavity Building Block. *Energy*, **35**, 3508-3516. <https://doi.org/10.1016/j.energy.2010.04.055>
- [44] Capelas de Oliveira, E. (2019) Integral Transforms. *Studies in Systems, Decision and Control*, **240**, 115-167. https://doi.org/10.1007/978-3-030-20524-9_4
- [45] Putri, E.R.M. and Surjanto, S.D. (2017) Performance of Gahver-Stehfest Numerical

- Laplace Inversion Method on Option Pricing Formulas. *International Journal of Computing Science and Applied Mathematics*, **3**, 71-76.
<https://doi.org/10.12962/j24775401.v3i2.2215>
- [46] Horváth, I., Talyigás, Z. and Telek, M. (2018) An Optimal Inverse Laplace Transform Method without Positive and Negative Overshoot—An Integral Based Interpretation. *Electronic Notes in Theoretical Computer Science*, **337**, 87-104.
<https://doi.org/10.1016/j.entcs.2018.03.035>
- [47] Kuznetsov, A. and Miles, J. (2022) On the Rate of Convergence of the Gaver-Stehfest Algorithm. *IMA Journal of Numerical Analysis*, **42**, 1645-1664.
<https://doi.org/10.1093/imanum/drab015>
- [48] Nellis (2009) Numerical Inverse Laplace Transform. E29: Section 3.4.7.
- [49] Jannot, Y. (2011) Metrologie Thermique. Lab. d’Énergétique Mécanique Théorique Appliquée, 6-97.
- [50] Mazieres, A., Trachman, M., Cointet, J., Coulmont, B. and Prieur, C. (2014) Deep tags: Toward a Quantitative Analysis of Online Pornography. *Porn Studies*, **1**, 80-95.
<https://doi.org/10.1080/23268743.2014.888214>
- [51] de Hoog, F.R., Knight, J.H. and Stokes, A.N. (1982) An Improved Method for Numerical Inversion of Laplace Transforms. *SIAM Journal on Scientific and Statistical Computing*, **3**, 357-366. <https://doi.org/10.1137/0903022>
- [52] Serrano, S., Barreneche, C. and Cabeza, L.F. (2016) Use of by-Products as Additives in Adobe Bricks: Mechanical Properties Characterisation. *Construction and Building Materials*, **108**, 105-111. <https://doi.org/10.1016/j.conbuildmat.2016.01.044>
- [53] Binici, H., Aksogan, O. and Shah, T. (2005) Investigation of Fibre Reinforced Mud Brick as a Building Material. *Construction and Building Materials*, **19**, 313-318.
<https://doi.org/10.1016/j.conbuildmat.2004.07.013>
- [54] Athiyamaan, V. and Ganesh, G.M. (2017) Statistical and Detailed Analysis on Fiber Reinforced Self-Compacting Concrete Containing Admixtures—A State of Art of Review. *IOP Conference Series: Materials Science and Engineering*, **263**, Article ID: 032037. <https://doi.org/10.1088/1757-899X/263/3/032037>
- [55] Ismaiel, M., Chen, Y., Cruz-Noguez, C. and Hagel, M. (2022) Thermal Resistance of Masonry Walls: A Literature Review on Influence Factors, Evaluation, and Improvement. *Journal of Building Physics*, **45**, 528-567.
<https://doi.org/10.1177/17442591211009549>
- [56] Imbga, B.K., Ouedraogo, E., Bayala, A., Ouedraogo, H., Ouattara, F. and Kieno, F. (2022) Characterization of Thermal and Mechanical Properties of Red Clay Mixed with Rice Straw for Thermal Insulation of Buildings. *American Journal of Energy Engineering*, **10**, 68-74.
- [57] Schöpfer, M.P.J., Abe, S., Childs, C. and Walsh, J.J. (2009) The Impact of Porosity and Crack Density on the Elasticity, Strength and Friction of Cohesive Granular Materials: Insights from DEM Modelling. *International Journal of Rock Mechanics and Mining Sciences*, **46**, 250-261. <https://doi.org/10.1016/j.ijrmms.2008.03.009>
- [58] Danso, H., Martinson, D.B., Ali, M. and Williams, J.B. (2015) Physical, Mechanical and Durability Properties of Soil Building Blocks Reinforced with Natural Fibres. *Construction and Building Materials*, **101**, 797-809.
<https://doi.org/10.1016/j.conbuildmat.2015.10.069>
- [59] Tonye Emmanuel, M. and Duval Roger, P.M. (2004) Caractérisation De Matériaux Locaux En.
- [60] Millogo, Y., Morel, J.C., Aubert, J.E. and Ghavami, K. (2014) Experimental Analysis

- of Pressed Adobe Blocks reinforced with *Hibiscus cannabinus* fibers. *Construction and Building Materials*, **52**, 71-78.
<https://doi.org/10.1016/j.conbuildmat.2013.10.094>
- [61] El-Sayed Ali, M. and Zeitoun, O.M. (2012) Discovering and Manufacturing a New Natural Insulating Material Extracted from a Plant Growing up in Saudi Arabia. *Journal of Engineered Fibers and Fabrics*, **7**, 88-94.
<https://doi.org/10.1177/155892501200700405>
- [62] Djadouf, S., Tahakourt, A., Chelouah, N. and Merabet, D. (2011) Étude de l'influence des ajouts (grignon d'olive et foin) sur les caractéristiques physico-mécanique de la brique de terre cuite. *Communication Science & Technologie*, **9**.
- [63] Demir, I. (2008) Effect of Organic Residues Addition on the Technological Properties of Clay Bricks. *Waste Management*, **28**, 622-627.
<https://doi.org/10.1016/j.wasman.2007.03.019>
- [64] Delot, P. (n.d.) Les adobes.
- [65] Benazzouk, A., Douzane, O., Mezreb, K., Laidoudi, B. and Quéneudec, M. (2008) Thermal Conductivity of Cement Composites Containing Rubber Waste Particles: Experimental Study and Modelling. *Construction and Building Materials*, **22**, 573-579. <https://doi.org/10.1016/j.conbuildmat.2006.11.011>
- [66] Lahouioui, M. (2019) Elaboration et évaluation des propriétés physico-thermiques et acoustiques de nouveaux éco-composites à base de bois de palmier.
- [67] Moretti, E., Belloni, E. and Agosti, F. (2016) Innovative Mineral Fiber Insulation Panels for Buildings: Thermal and Acoustic Characterization. *Applied Energy*, **169**, 421-432. <https://doi.org/10.1016/j.apenergy.2016.02.048>